MATEC Web of Conferences **14**, 18001 (2014)
DOI: 10.1051/matecconf/20141418001

First principles study of structural stability and site preference in Co_3 (W,X)

Sri Raghunath Joshi[a], K.V. Vamsi, and S. Karthikeyan

Department of Materials Engineering, Indian institute of Science, Bangalore 560012, India

Abstract. Since the discovery [1] of γ' precipitate ($L1_2$ – Co_3(Al, W)) in the Co-Al-W ternary system, there has been an increased interest in Co-based superalloys. Since these alloys have two phase microstructures ($\gamma + \gamma'$) similar to Ni-based superalloys [2], they are viable candidates in high temperature applications, particularly in land-based turbines. The role of alloying on stability of the γ' phase has been an active area of research. In this study, electronic structure calculations were done to probe the effect of alloying in Co_3W with $L1_2$ structure. Compositions of type Co_3(W,*X*), (where X/Y = Mn, Fe, Ni, Pt, Cr , Al, Si, V, W, Ta, Ti, Nb, Hf, Zr and Mo) were studied. Effect of alloying on equilibrium lattice parameters and ground state energies was used to calculate Vegard's coefficients and site preference related data. The effect of alloying on the stability of the $L1_2$ structure *vis a vis* other geometrically close packed ordered structures was also studied for a range of Co_3X compounds. Results suggest that the penchant of element for the W sublattice can be predicted by comparing heats of formation of Co_3X in different structures.

1. Introduction

Superalloys are widely used in gas-turbine industry for land-based power generation systems as well as in aircraft engines. For power generation applications, where the fuel is not as "clean" as in the case of aircraft engines, sulphidization resistance is an important criterion for material selection. In this regard Co-base superalloys are promising candidates for land-based turbine applications [3]. Interest in Co-base alloys has been renewed since the discovery of $L1_2$ structured cuboidal precipitates of the composition Co_3(Al,W) in the Co-Al-W system [1]. In this class of Co-base alloys, the microstructure consists of $L1_2$(γ') precipitates of composition Co_3(Al, W) in a Co-rich fcc (γ) matrix [1,4–6] and in this aspect, the microstructure is akin to Ni-base superalloys typically used in gas turbine applications [2]. Single crystal [7] and polycrystalline [4,5] Co-Al-W base superalloys have been tested for mechanical properties such as elastic moduli [7], high temperature creep resistance and ductility [8]. It has been shown that Co-base superalloys fared similar to some Ni-base superalloys at 900 °C [4]. Pyczak et al. [9] have shown that the deformation microstructures in Co-Al-W alloys are also similar to the ones in Ni base superalloys.

Given that these materials are relatively immature, it is important to understand the role of alloying elements on phase stability. In this context, a keen area of research has been to find quaternary alloying additions that would enhance the stability of the γ' phase and widen the composition domain where it is stable [10,11]. This is particularly important since the phase is stable only when the composition is close to $Co_3(Al_{0.5}W_{0.5})$ [12]. An understanding of alloying effects on phase stability is also expected to assist in designing alloys with optimum volume fraction of γ' so that the desired mechanical properties are met. To expedite this effort, many researchers have used first principles calculations based on density functional theory, to generate baseline data and to support experimental alloy design [10]. These efforts have focused primarily on predicting equilibrium lattice parameters [12], elastic constants [12,13] and ideal strength of $L1_2$–Co_3(Al,W), [14] and to understand site preference [15,16] of various alloying elements in γ'. In this study we contribute to this effort by computing the effect of several alloying elements–Mn, Fe, Ni, Pt, Cr , Al, Si, V, W, Ta, Ti, Nb, Hf, Zr and Mo–on lattice parameter of Co_3W using first principles electronic structure methods. In this study, we also explore site preference of these alloying elements. In these calculations, the base alloy was chosen to be Co_3W (in $L1_2$) and not Co_3Al. This is because Co_3Al is not a stable compound formed in the Co-Al phase diagram, whereas Co_3W is stable in the DO_{19} structure (and structurally similar to $L1_2$). We attribute the occurrence of $L1_2$–Co_3(Al,W) to the $L1_2$ stabilizing effect of Al in Co_3W. The site preference data and Vegard's parameters are expected to be useful for identifying other stabilizers of the $L1_2$ phase and for designing alloys with desired misfit.

While Co–Al–W base superalloys systems remain the most promising for the presence of an $L1_2$ based precipitate, alternative candidates for γ' other than Co_3(Al,W) have not been well explored. Since $L1_2$ phases

[a] Corresponding author: karthik@materials.iisc.ernet.in

have been reported in Co–Ti [17], Co–Ta [18] and Co–V [19,20] systems, it is imperative that the possibility of stabilizing other Co_3X type compounds in $L1_2$ structure be explored. In this context, Xu et al. [21] have studied the structural stability of Co_3X compounds (X =Ti, Ta, V, W and Al) in $L1_2$ as well as in DO_{19} structures. They have shown that Ti, Ta and V are strong $L1_2$ stabilisers whereas W and Al are DO_{19} stabilisers. Additionally, Omori et al. [22] have shown that heats of formation of Co_3X compounds in $L1_2$ and DO_{19} structures can give vital and indirect information about partitioning behaviour of alloying elements to various phases in a Co–Al–W system. Clearly, calculations in Co_3X not only help explore novel $L1_2$ compositions, but also provide insights for stabilizing $L1_2$–Co_3(Al,W). Moreover, it has been shown [23,24], that the structural energy of Ni_3X in different structures can be correlated well with various planar fault energies. A similar effort in Co_3X will provide insights into the role of alloying on fault energies in Co–Al–W, Co–Al–W-X and Co-X systems. In this context, the second aim of this work is to compute the energy of various Co_3X compounds in geometrically close packed structures – $L1_2$, DO_{19}, DO_{22}, DO_{24}, and DO_a for various alloying elements. In current literature, this data is available only for a limited set of alloying elements and only in $L1_2$ and DO_{19} structures.

In the first part of this paper, we describe the computational methodology employed. Subsequently, site preference and Vegard's coefficients of various alloying elements in Co_3W, and structural stability of Co_3X in different structures is presented. In the final section, the possibility of predicting site preference of X in Co_3W from the stability of Co_3X is explored.

2. Method of calculation

Density functional theory calculations were performed using Vienna Abinitio Simulation Package^{TM} (VASP 4.6) [25,26] within the MedeA environment [27]. Projected Augmented Wave method [28,29] was used with generalised gradient approximation based pseudo-potentials where parameterization was in the scheme of Perdew and Wang (PW – GGA) [30]. Electrons in the outermost shell were only considered for calculations involving most elements except Mo, Cr and Nb where the semicore p-shell electrons were also taken into consideration. The electron wave functions were expanded using a plane wave basis set with a cutoff energy of 550 eV. The Brillouin zone was divided using a K-point spacing of 0.1 Å^{-1}. A Methfessel-Paxton type smearing (of 1^{st} order) was applied to the wave function over a width of 0.1 eV. The system size was of 32 atoms. Local atomic relaxation was allowed in all cases. All calculations were run until a convergence of 10^{-5} eV was attained in total energy and the forces on individual atoms were less than 0.02 eV/Å.

In the first set of calculation, site preference and Vegard's coefficients of alloying elements in $L1_2$-Co_3W was computed. With $L1_2$-Co_3W as the reference, alloying elements were added to the Co and W sublattices to result in compositions of $(Co_{23}X)W_8$ and $Co_{24}(W_7X)$ respectively. Equilibrium lattice parameters as well as ground state total energies were obtained for these compositions. From these calculations, site preference (with reference to W) was estimated by computing the enthalpy change, ΔE_3 associated with the following equation which involves swapping of X in the Co sublattice with a W atom in the W sublattice:

Table 1. Lattice parameters a', $b'$and c' used to constrain DO_{19}, DO_{22}, DO_{24} and DO_a to the equilibrium lattice parameters of $L1_2$.

	DO_{19}	**DO_{22}**	**DO_{24}**	**DO_a**
a'/a_{L1_2}	$\sqrt{2}$	1	$\sqrt{2}$	$\sqrt{2}$
b'/a_{L1_2}	$\sqrt{2}$	1	$\sqrt{2}$	$\sqrt{4/3}$
c'/a_{L1_2}	$\sqrt{4/3}$	2	$4\sqrt{1/3}$	$\sqrt{3/2}$

$$Co_{24}W_8 + Co_{23}XW_8 \rightarrow Co_{24}W_7X + Co_{23}WW_8 \quad (1)$$

$$\Delta E_3 = \mathrm{E}^{L12}_{Co_{24}(W_7X)} + \mathrm{E}^{L12}_{(Co_{23}W)W_8} - \mathrm{E}^{L12}_{(Co_{23}X)W_8} - \mathrm{E}^{L12}_{Co_{24}W_8} \quad (2)$$

$\mathrm{E}^{L12}_{Co_{24}(W_7X)}$, $\mathrm{E}^{L12}_{(Co_{23}W)W_8}$, $\mathrm{E}^{L12}_{(Co_{23}X)W_8}$ and $\mathrm{E}^{L12}_{Co_{24}W_8}$ are the ground states energies of the compositions indicated in the subscript and in $L1_2$ structure. Positive values of ΔE_3 suggest a weaker preference (than W) for the Co sublattice. Using the equilibrium lattice parameters of $(Co_{23}X)W_8$ and $Co_{24}(W_7X)$ and comparing with that of Co_3W, all in $L1_2$ structure, Vegard's coefficient (γ) of these alloying additions in different sublattices was calculated:

$$\Upsilon_W = \frac{a_{Co_{24}(W_7X)} - a_{Co_3W}}{\left(\frac{1}{8}\right) a_{Co_3W}} \quad (3)$$

$$\Upsilon_{Co} = \frac{a_{(Co_{23}X)W_8} - a_{Co_3W}}{\left(\frac{1}{24}\right) a_{Co_3W}} \quad (4)$$

where $a_{Co_{24}(W_7X)}$ and $a_{(Co_{23}X)W_8}$ are the equilibrium lattice parameters (for a 4 atom unit cell) for X in W and Co sublattices respectively and a_{Co_3W} is the equilibrium lattice parameter of Co_3W.

For the second part of the study, Co_3X compounds were simulated in $L1_2$, DO_{19}, DO_{22}, DO_{24}, and DO_a. Two sets of calculations were done. In the first set, the lattice parameters were adjusted for each structure so that it achieved the lowest ground state energy for that structure (i.e., fully relaxed). From this, equilibrium lattice parameters were calculated for Co_3X in all structures. In the second set of calculations, Co_3X type structures in DO_{19}, DO_{22}, DO_{24} and DO_a were constrained to lattice parameters which resulted in the same atomic volume, coordination, and bond lengths as found in the equilibriated Co_3X in $L1_2$, and ground state energy was evaluated. Table 1 shows the appropriate choice of constrained lattice parameters for each structure.

Cohesive energies and heats of formation were calculated for these compounds using:

$$\mathrm{E}^{S}_{c,Co_3X} = \frac{\mathrm{E}^{S}_{Co_3X} - 3\mathrm{E}^{iso}_{Co} - \mathrm{E}^{iso}_{X}}{4} \quad (5)$$

$$\mathrm{H}^{S}_{c,Co_3X} = \frac{\mathrm{E}^{S}_{Co_3X} - 3E^{hcp}_{Co_1} - E^{native}_{X_1}}{4} \quad (6)$$

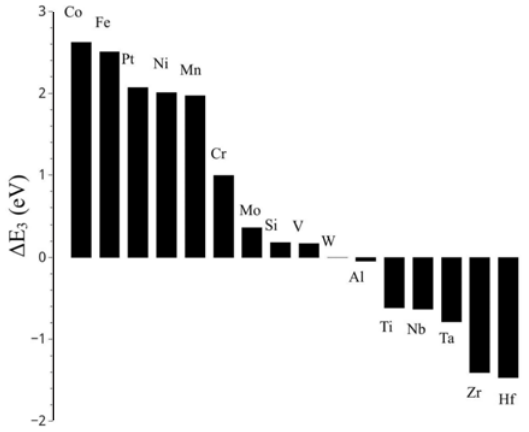

Figure 1. – Site preference behaviour as evaluated from ΔE_3 for different alloying elements.

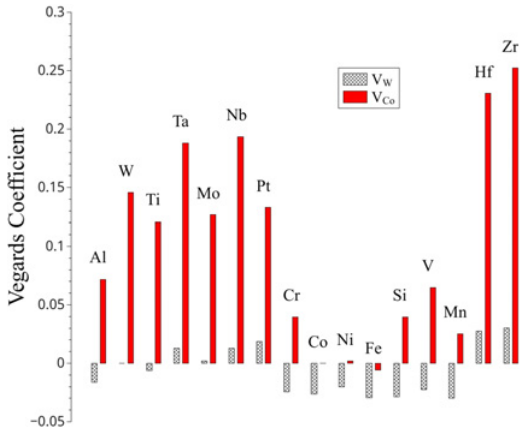

Figure 2. Vegards coefficients of different alloying elements in the two sublattices of $L1_2$–Co_3W.

where E^S_{c,Co_3X} is the cohesive energy of Co_3X in structure S. E^{iso}_{Co} and E^{iso}_X are the ground state energies of Co and X in an isolated state. H^S_{c,Co_3X} is the heat of formation of Co_3X in structure S, $E^{hcp}_{Co_1}$is the ground state energy of one atom of Co in hcp structure, and $E^{native}_{X_1}$ is the ground state energy of one atom of X in its native structure (as indicated in Table 2).

3. Results & Discussion

3.1. Alloying effects

Figure 1 shows the values of ΔE_3 for several alloying elements. ΔE_3 is an indicator of the element's preference for a sublattice (Co or W) in Co_3W. Positive values of $\Delta E_3$for an element X suggest that the element has a greater affinity (than W) to go to the Co sublattice in Co_3W. Negative values of ΔE_3suggest that the alloying element prefers the W sublattice even more than W does. Thus elements with negative ΔE_3strongly prefer W sublattice. Positive ΔE_3 does not imply a preference for the Co-lattice. Instead what it means is that the alloying element has a greater affinity (than W) to go to the Co sublattice in Co_3W. From this one can conclude that Hf, Zr, Ti, Ta, Nb and Al prefer the W sublattice more so than W, whereas, elements with high positive values such as Pt, Fe, Ni, Mn are likely to occupy the Co sublattice. Elements with small positive values (i.e. Cr, Mo, V, Si) are expected to equipartition to different extents between the two sublattices.

Figure 2 shows the Vegard's coefficients for various elements in the two sublattices. It is observed that that $\Upsilon_{Co}$for most alloying elements is positive, given the small size of the Co atom. This suggests that their presence in the Co sublattice would result in a significant increase in γ' lattice parameter. In comparison, Υ_W takes on both positive and negative values, given the intermediate size of the W atom.

Unlike Ni base superalloys, Co–Al–W based superalloys have a positive misfit, i.e, $a_{\gamma'} > a_\gamma$ by ∼0.5%. This can result in high energy semi-coherent γ/γ' interfaces with a tendency to coarsen rapidly; resulting in a loss of mechanical properties. In this context, alloying additions that increase the lattice parameter of γ and decrease that of γ' are attractive. While Vegard's coefficients in γ were not calculated in this study, one can use site preference data from Fig. 1 in conjunction with the Vegard's coefficient, to predict if an alloying element would reduce the lattice parameter of γ'; if such an alloying element goes to the sublattice of its thermodynamic choice, then in that sublattice it must have a negative Vegard's coefficient. This criterion limits the possible candidates to Cr, V, Si, Al and to a minor extent, Fe.

In accordance with Hume-Rothery rules [31], for an alloying element to prefer a sublattice it has to be similar to the primary atom in that sublattice in its size and in its chemical nature. Vegard's coefficient is an appropriate measure of the size difference between the alloying element and "solvent" atom. The chemical similarity between the solvent atom and the alloying addition has been previously related to the number of valence electrons in the two elements [12]. However, since most alloying elements considered in this study are transition metals and have multiple valences, we have instead used the electronegativity parameter (Φ^*), proposed by Miedema et al. [33] as a measure of chemical similarity between the alloying element and the matrix. In Fig. 3, various alloying elements have been mapped in the space of Vegard's coefficient (in specific sublattice) and the difference in Φ^* between X and the solvent atom in that sublatice; Fig. 3a is for the Co sublattice, while 3b is for the W sublattice. In these figures, the radius of the circles is proportional to the absolute value of ΔE_3. Additionally positive values of ΔE_3 are color coded red and negative ones are coded blue. Larger discontinuous blue circles indicate elements with a strong preference for the W sublattice, while large continuous red circles indicate a strong preference for the Co sublattice.

From these figures, it can be seen that there is a cluster of the elements that prefer the Co sublattice and a second cluster of elements–diametrically on the other side of the map–that prefer the W sublattice. In the map for the Co sublattice, it is observed that elements that strongly partition to the Co sublattice (i.e., large red circles), are clustered around (0, 0) and are thus similar in size and chemical nature to Co. Likewise, in the map for the W

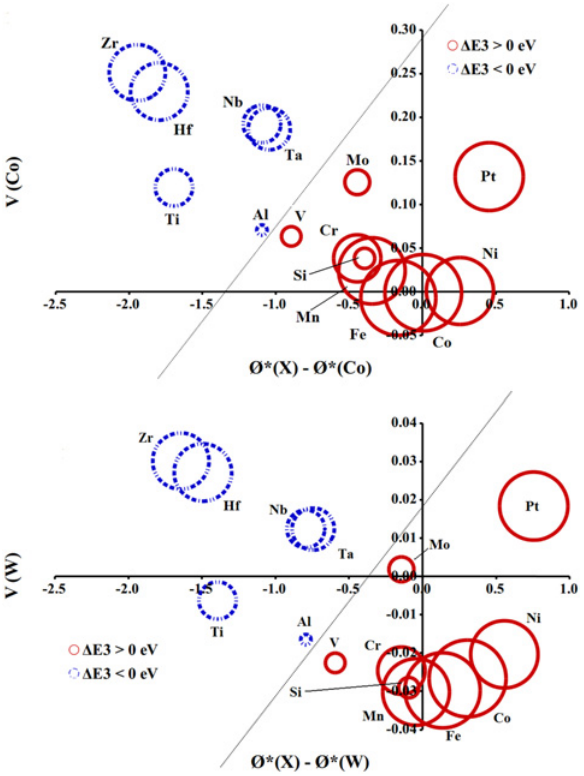

Figure 3. A map of electronegativity difference versus Vegards coefficient of an alloying element in different sublattices–Co sublattice (top) and W sublattice (bottom). The color and size of the circles correspond to the sign and magnitude of ΔE_3.

sublattice, the elements closest to W (0, 0) are Cr and Mo, both of which are in the same group as W. In these figures, we have indicated a crude demarcation between the elements that prefer the W sublattice and others. These maps can be useful in designing alloys. For instance, in the map for Co sublattice, it can be concluded that for elements to strongly prefer the W sublattice, they have to be deep in the second quadrant (x<<0, y>>0). Since the Miedema electronegativity is known for most metals in the periodic table, and a rough estimate for the Vegard's coefficient can also be derived from the difference in the metallic radii (also readily available across the periodic table) of the metal and cobalt, the site preference of any metal in Co_3W can be predicted approximately. For instance, it is predicted that Y and Sc will prefer the W sublattice even more than Zr and Hf. It will be interesting to check if this prediction is borne out.

3.2. Structural stability

The cohesive energies and heats of formation of Co_3X type compounds computed in DO_{19}, DO_{22}, DO_{24} and DO_a structures (constrained and fully relaxed) are compared with those of $L1_2$ in Table 2. The heats of formation of these compounds are in good agreement with computational results of Xu et al. [21] and Omori et al. [22] as well as with experimental results where available. This validates the procedure employed for calculating these parameters. Cohesive energy of Co_3X (X=Ti, Ta, Al, W and V) has been reported by Xu et al. [21]. However,

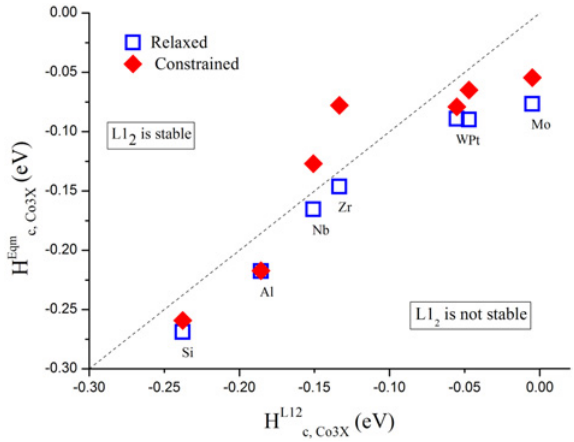

Figure 4. Alloying elements are mapped in the H^{L12}_{c,Co_3X} and H^{Eqm}_{c,Co_3X} space. Elements that lie southeast of the indicated line (of slope 1) are unstable in $L1_2$ and those that lie in the northwest are stable in $L1_2$.

cohesive energies reported in their work appear to be unreasonably low compared to our results. In fact, their values for cohesive energy for Co_3W in DO_{19} and Co_3Ti in $L1_2$ are not different from experimentally determined cohesive energy for W in BCC structure [34]. This is improbable since this would imply that Co_3W, Co_3Ti and W would have similar melting points, which is known not to be true. Note: melting points of most metals and intermetallics scale linearly with cohesive energy [34]. In contrast, the cohesive energy values derived in this work are reasonable and scale well with known melting points of these intermetallics.

From the cohesive energy data, it is noted that Co_3X (X=Ti, Ta, Hf, Mn and V) is most stable in $L1_2$ structure for fully relaxed calculations, while Co_3Si is most stable in DO_{22} and Co_3Al is most stable in DO_a. For all other alloying elements, DO_{19} is the stablest structure in the fully relaxed condition.

A comparison of the heat of formation of H^{L12}_{c,Co_3X} against that in its equilibrium structure H^{Eqm}_{c,Co_3X} reveals important features. Such a map is shown in figure 4. The blue rectangles correspond to the H^{L12}_{c,Co_3X} and H^{Eqm}_{c,Co_3X}. values of alloying elements. Only those elements are shown whose values lie to the right of the unity line, i.e., whose equilibrium structure has a lower heat of formation and is more stable than $L1_2$. Alloying additions whose values lie closer to the line (such as Nb and Zr) have comparable values of H^{Eqm}_{c,Co_3X} and H^{L12}_{c,Co_3X} and it is reasonable to assume that Co_3Nb and Co_3Zr can be stabilized in $L1_2$ with relative ease perhaps by alloying. In contrast, stabilizing Co_3Mo in $L1_2$ may be difficult since Mo is further away from the line. This argument has also been put forth by Omori et al. [22]. Another interesting feature emerges by comparing the heat of formation, H^{L12}_{c,Co_3X} against that in the equilibrium structure constrained to $L1_2$ dimensions, i.e., $H^{Eqm,constr.}_{c,Co_3X}$. These trends are also shown in Fig. 4. The red diamonds are a comparison between H^{L12}_{c,Co_3X} and $H^{Eqm,constr.}_{c,Co_3X}$. Here it is seen that by constraining

Table 2. Cohesive energies and heats of formation of Co_3X type compounds in different structures, (fully relaxed and constrained to $L1_2$ lattice parameters). The cohesive energies of these compounds in the constrained structures are in parenthesis below. The lowest value of the cohesive energy, for each compound is highlighted in bold face font.

		Cohesive Energy of Co_3X (eV / atom)					Heat of formation of Co_3X (kJ / mol)			
	Native Structure						$L1_2$		DO_{19}	
X		$L1_2$	DO_{19}	DO_{22}	DO_{24}	DO_a	Calc.	Ref	Calc.	Ref
Al	FCC	−4.9650	−4.9901 (−4.9891)	−4.9858 (−4.9819)	−4.9768 (−4.9764)	**−4.9969** (−4.9965)	−17.92	−17.97 [22]	−20.34	−20.41 [22]
W	BCC	−6.0738	**−6.1077** (−6.0977)	−6.0451 (−6.0440)	−6.0916 (−6.0838)	−6.0836 (−−6.0787)	−5.33	−4.81 [22]	−8.60	−8.07 [35] *expt*
Ti	HCP	**−5.5573**	−5.5260 (−5.5087)	−5.5055 (−5.4987)	−5.5378 (−5.5324)	−5.5178 (−5.4855)	−24.32	−25.88 [22]	−21.30	−22.67 [22]
Ta	BCC	**−6.2733**	−6.2662 (−6.2318)	−6.1934 (−6.1898)	−6.2725 (−6.2559)	−6.2104 (−6.2016)	−24.16	−23.44 [22]	−23.49	−22.92 [22]
Mo	BCC	−5.4762	**−5.5295** (−5.5257)	−5.4832 (−5.4588)	−5.5010 (−5.5001)	−5.5215 (−5.5025)	−0.48	−0.549 [36]	−5.62	−5.30 [37] *expt*
Nb	BCC	−5.7852	**−5.7999** (−5.7614)	−5.7246 (−5.7208)	−5.7953 (−5.7756)	−5.7516 (−5.7422)	−14.55	−14.42 [22]	−15.97	−15.81 [22]
Pt	FCC	−5.3380	**−5.3808** (−5.3559)	−5.3357 (−5.3355)	−5.3548 (−5.3532)	−5.3662 (−5.3626)	−4.54		−8.67	
Cr	BCC	−4.8739	**−4.9337** (−4.9122)	−4.8823 (−4.8769)	−4.8902 (−4.8879)	−4.9234 (−4.9159)	4.84	2.36 [22]	−0.94	−0.83 [22]
Ni	FCC	−5.1977	**−5.2249** (−5.2226)	−5.1973 (−5.1965)	−5.2089 (−5.2084)	−5.2208 (−5.2198)	0.48	0.50 [22]	−2.15	−2.06 [22]
Fe	BCC	−5.0213	**−5.1650** (−5.1223)	−5.0423 (−5.0405)	−5.0187 (−5.0185)	−5.0571 (−5.0526)	17.41	17.29 [22]	3.55	3.39 [22]
Si	Diamond cubic	−5.2979	−5.3191 (−5.3150)	**−5.3291** (−5.3194)	−5.3047 (−5.2939)	−5.3244 (−5.3213)	−22.93		−24.98	
V	BCC	**−5.4281**	−5.4262 (−5.4175)	−5.3763 (−5.3716)	−5.4251 (−5.4212)	−5.1727 (−4.8501)	−16.70	−17.05 [22]	−16.51	−16.79 [22]
Mn	BCC	**−4.8518**	−4.8014 (−4.7951)	−4.8040 (−4.7977)	−4.8040 (−4.7916)	−4.8114 (−4.7880)	0.32	3.52 [22]	5.19	7.61 [22]
Hf	HCP	**−5.8218**	(−5.8129) (−5.7606)	−5.7620 (−5.7554)	−5.8133 (−5.7910)	−5.8156 (−5.7832)	−21.45		−20.59	
Zr	HCP	−5.6057	**−5.6184** (−5.5499)	−5.5633 (−5.5572)	−5.6090 (−5.5796)	−5.6031 (−5.5923)	−12.89		−14.11	

Co_3Nb and Co_3Zr, $L1_2$ structure becomes stabler than its unconstrained equilibrium structure. This is interesting because it suggests that Co_3X can be stabilized in $L1_2$ if its dimensions are constrained. One possible source of constraint could be the Co matrix itself from which the γ' precipitates. Another possible means of constraining Co_3X may be by alloying. Thus this suggests that there may be possible means of stabilizing many Co_3X compounds in $L1_2$.

3.3. Structural stability and site preference in Co_3W

It is worthwhile considering if one can use H^{L12}_{c,Co_3X} to predict how the alloying element X would behave when introduced into Co_3W. In Fig. 5, ΔE_3 is plotted as a function of $H^{L12}_{c,Co_3X} - H^{L12}_{c,Co_3W}$. Reasonable correlation is observed; if for an element X, $H^{L12}_{c,Co_3X} < H^{L12}_{c,Co_3W}$, then it is highly likely that the element will prefer the W sublattice when introduced in Co_3W. Since H^{L12}_{c,Co_3X} calculations involve small systems (4 atoms), these are computationally much easier than computations of ΔE_3 which are expensive given that at least four 32-atom calculations involving atomic relaxation have to be made for each alloying element. In this context, computation of $H^{L12}_{c,Co_3X} - H^{L12}_{c,Co_3W}$ for a wide range of alloying elements is suggested as an ideal means of rapidly screening elements for their potential to enter the W sublattice in Co_3W.

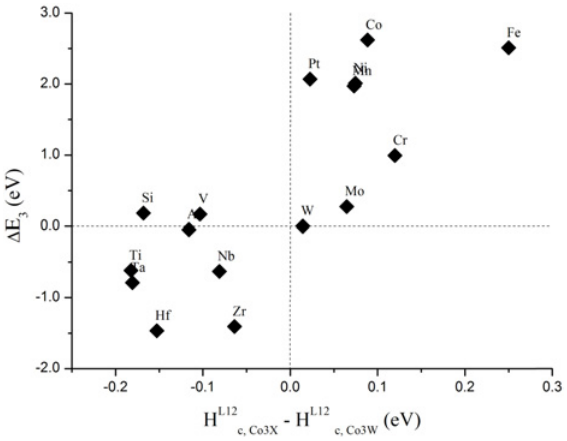

Figure 5. ΔE_3 plotted as a function of $H^{L12}_{c,Co_3X} - H^{L12}_{c,Co_3W}$.

4. Conclusions

Site preference and Vegard's coefficients of several alloying elements were probed in $L1_2 - Co_3W$. It is found that site preference is strongly dependent of size mismatch and electronegativity difference between X, and Co and W. The stability of Co_3X compounds was probed in different structures and it was shown that heat of formation could be used to predict if Co_3X itself can be stabilized in $L1_2$ and if X will prefer a W site or a Co site if added to Co_3W.

The authors acknowledge the support of Department of Science and Technology, Government of India.

References

[1] J. Sato, T. Omori, K. Oikawa, I. Ohnuma, R. Kainuma and K. Ishida, Science, **312**, 90 (2006)
[2] R, C. Reed, *The Superalloys: Fundamentals and Applications*, Cambridge University Press (2006)
[3] A. M. Beltran In: *Superalloys II*. New york (NY): Wiley; 135 (1987)
[4] M. S. Titus, A. Suzuki, T. M. Pollock, *Proceedings of 12th international symposium on Superalloys 2012*, 823 (2012)
[5] A. Bauer, S. Neumeie, F. Pyczak, M. Göken, *Proceedings of 12th international symposium on Superalloys 2012*, 695 (2012)
[6] A. Suzuki, T. M. Pollock, Acta. Mater. **56**, 1288 (2008)
[7] K. Tanaka, T. Ohashi, K. Kishida, and H. Inui, Appl. Phy. Lett., **91**, 181907 (2007)
[8] K. Shinagawa, T. Omori, K. Oikawa, R. Kainuma and K. Ishida Scri. Mater., **61**, 612 (2009)
[9] F. Pyczak, A. Bauer, M. Göken, S. Neumeier, U. Lorenz, M. Oehring, N. Schell, A. Schreyer, A. Stark, F. Symanzik, Mater..Sci. Eng., A **571**, 13 (2013)
[10] M. Chen and C. Y. Wang J. Appl Phy., **107**, 093705 (2010)
[11] M. Chen and C. Y. Wang Scri. Mater., **60**, 659 (2009)
[12] A. Mottura, A. Janotti, T. M. Pollock, *Proceedings of 12th international symposium on Superalloys* 685 (2012)
[13] Q. Yao, H. Xing, and J. Sun, Appl. Phy. Lett., **89**, 161906 (2006)
[14] C Jiang, Scri. Mater., **59**, 1075 (2008)
[15] Y. J. Wang and C. Y. Wang, Appl. Phy. Lett., **94**, 261909 (2009)
[16] M. Chen and C. Y. Wang, J. Appl. Phy., **107**, 093705 (2010)
[17] M. Chen and C. Y. Wang, Scri. Mater., **60**, 659 (2009)
[18] JM Blaise, P. Viatour and J. M. Drapier *Cobalt (Engl Ed)* **49**, 192 (1970)
[19] J. M. Drapier, J. L. De Brouwer and D. Coutsouradis *Cobalt (Engl Ed)* **27**, 59 (1965)
[20] E. T. Peters and L. E. Tanner, Trans. Metall. Soc. AIME **233**, 2126 (1965)
[21] Y. Aoki, K. Asami and M. Yamamoto, Phys Stat. Sol. (A)., **23**, 167 (1974)
[22] W. W. Xu, J. J. Han, Z. W. Wang, C. P. Wang, Y. H. Wen, X. J. Liua and Z. Z. Zhu Intermetallics **32**, 303 (2013)
[23] T. Omori, K. Oikawa, J, Sato, I. Ohnuma, U. R. Kattner, R. Kainuma and K. Ishida Intermetallics **32**, 274 (2013)
[24] K V Vamsi and S Karthikeyan, *Proceedings of the 12th international symposium on Superalloys* 0521 (2012)
[25] K. V. Vamsi and S. Karthikeyan, Unpublished
[26] G. Kresse and J. Furthmiller, Phys Rev B **54**, 11169 (1996)
[27] G. Kresse and J. Furthmiller J. Comp Mater Sci **6**, 15 (1996)
[28] MedeA Version 2.6.6 Materials Design Inc, Angel Fire, NM, USA (2009)
[29] P. E. Blochl, Phys Rev B **50**, 17953 (1994)
[30] G. Kresse and D. Joubert Phys Rev B **159**, 1758 (1999)
[31] J. P. Perdew, K. Burke and M. Ernzerhof Phys Rev Lett **77**, 3865 (1996)
[32] W. Hume-Rothery and G. V. Raynor *The Structure of Metals and alloys,* The Institute of Metals (1956)
[33] A. R. Miedema, Journal of the Less-Common Metals **32**, 117 (1973)
[34] W. Pfeiler *Alloy Physics* Wiley-VCH Verlag GmbH & Co. (2007)
[35] T. N. Rezukhina and T. A. Kashina, J. Chem Thermodynamics **8**, 513 (1976)
[36] K. Oikawa, U. R. Kattner, J. Sato, T. Omori, M. Jiang, K. Anzai and K. Ishida Materials Transactions **53**, 1425 (2012)
[37] L. Brewer, R. H. Lamoreaux, R. Ferro, R. Ma razza and K. Girgis, *Molybdenum* IAEA **7**, 123 & 231 (1980)